http://dx.doi.org/10.21622/MARLOG.2023.12.1.213
Vol. 12, Iss. 1, August 2023

Hydrodynamic Analysis of Ship Manoeuvrability at Ports using CFD

T. Tezdogan [1], D. Kim [2], and A. Incecik [3]

[1] Department of Civil, Maritime and Environmental Engineering, University of Southampton, Southampton
[2], [3] Department of Naval Architecture, Ocean and Marine Engineering, University of Strathclyde, Glasgow

E-Mail: t.tezdogan@soton.ac.uk, daejeong.kim@strath.ac.uk, atilla.incecik@strath.ac.uk

1. ABSTRACT: The way a ship moves in restricted waters is significantly different from how it moves in open waters due to the impact of limited depth conditions. This is because ships often operate in shallow water areas like ports or harbours. To understand these effects on ship manoeuvrability, the manoeuvrability of the KRISO Container Ship (KCS) model was studied at ports using unsteady Reynolds-Averaged Navier-Stoked computations combined with 6 degree-of-freedom (DOF) rigid body motion equations. The study used an adaptive dynamic mesh approach to allow the vessel to move freely and for the rudder to be controlled. Simulation tests were performed at ports modelled as restricted waters with varying water depth to draft ratios, and results were partially validated with experimental data. The findings showed that the ship's forward movement, lateral movement, and tactical diameter increased as the water depth to draft ratio decreased, linked to the complex interactions between the hull wake, boundary layer, propeller, vortex, and bottom of the seabed.

Keywords: *CFD, Reynolds-Averaged Navier-Stokes equations solver, Ship maneuverability, Restricted waters.*

2. INTRODUCTION

The growing size of ships has highlighted the need to understand how they maneuver in shallow water (Tezdogan et al., 2016). Navigation in shallow water is common for ships, especially when approaching harbors or ports. Some nearshore and open-sea areas can also be considered restricted waterregionswithlimiteddepthof the water. Proper decision-making about ship maneuvering actions requires a good understanding of a ship's maneuverability in shallow water by those in charge of navigation safety. However, available information on ship maneuvering is usually limited to deep water, obtained through full-scale sea trials or model-scale experiments, in compliance with International Maritime Organization (IMO) standards. Although these provide information on a ship's maneuverability in deep unrestricted water, they do not offer practical insights into maneuvering in shallowwater,whichcan differ significantly. This study aims to address this gap by investigating ship maneuvering performance in restricted waters such as ports using an unsteady Reynolds-Averaged Navier Stokes (URANS) method.

In this work reported in this paper, the turning ability of the KRISO Container Ship model in restrictedwaterportsisanalyzed.The focus is on the maneuvering indices and hydrodynamic loads related to the turning movements. The study also evaluates the various hydrodynamic phenomena that occur during the maneuver to provide a better understanding of the turning behavior. As a result, this research could be beneficial in comprehending the complete maneuverability of a container ship model in various shallow water port environments. It should be noted that the full version of this paper was published in Applied Ocean Research (Kim et al., 2022) by the same authors group. The results presented in the subsequent sections were adapted from the above-mentioned study.

3. METHODOLOGY

The methodology used in this study is outlined in this section, alongside a thorough explanation of the process in subsequent parts. The goal of the research is to investigate the maneuvering behaviors of the KCS in various shallow waters.The technique is comprised of four steps : **1)**"goalandscope", **2)** "numerical modeling", **3)** "execution of free-running simulations", and **4)** "results analysis". The process is depicted in a flow chart (Fig. 1) and is based on the methodology from the researchers' previous work (Kim et al., 2021a), adjusted to meet the objectives of this study. Step 1 defines the whole purpose and scale of the analysis. The second step outlines the numerical modeling aspect ofthe free-running CFD model. The third step involves conducting 'free-running' maneuvers using the Computational Fluid Dynamics model established in previous steps. The final step showcases and discusses the results obtained from the CFD simulations, with a focus on the connection between the vessel's turning operation and depths of the water.

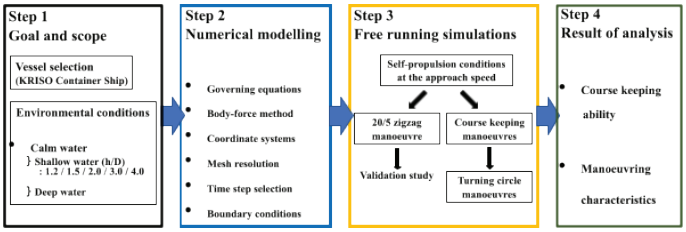

Figure 1: Suggested research procedure for the Computational Fluid Dynamics 'free-running' models

3.1.Step 1:"Goal and scope"

The objective of this work is to give a thorough knowledge of the impact of restricted water depth on ship maneuverability. This research will focus on:

1. Creating a numerical standard for 'free-running' maneuvers in restricted water
2. Validating the Computational Fluid Dynamic model using the results from the available tanks testing
3. Conducting numerical simulations and analyzing the effects of shallow water on ship maneuverability (such as "course keeping" and "turning" abilities)
4. Providing suggestions for future work, taking into account the limitations of the current research.

The study conducted numerical simulations for the containership model, which was created by KRISO and had a scale factor of 75.24. The model was equipped with a "semi-balanced rudder" andan "actuator disk". Table 1 provides the main features of the geometry. The work considered 7 different cases to be modelled in Computational Fluid Dynamics, as shown in Table 2 and Figure 3. The first case (Case 0) was a 20/5 modified zigzag maneuver in shallow water with a h/D ratio of 1.2, and the experimental results were used as a benchmark for validation. The following cases (Case 1-6) were two characteristic 'free-running' maneuvers ("course-keeping" and "standard turning") in different h/D ratios (1.2, 1.5, 2.0, 3.0, 4.0, and deep water). The first step concerned completing "self-propulsion" at the advancing speed and maintaining a constant revolution speed of the actuator disk. Then, the course-keeping maneuvers were started from the "self-propulsion" condition, using a rudder controller to control the 'rudder deflection' angle. Finally, the standard turning circle maneuvers were performed to assess the restricted water effects on the ship's turning behavior.

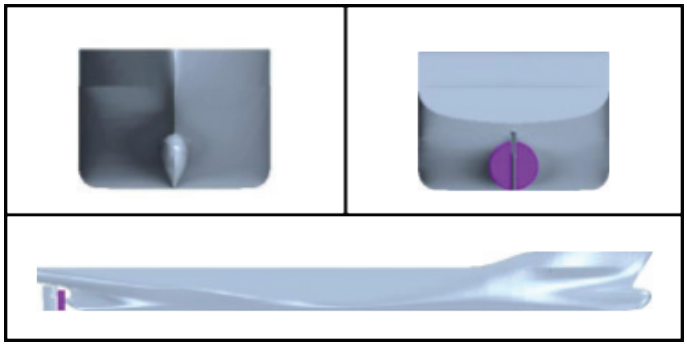

Figure 2: The containership model in question with a "semi balanced rudder" and an "actuator disk"

Table 1. The main dimensions of the containership model in question

Main particulars	Symbols	Model scale (1:75.24)
Length between the perpendiculars	$L_{BP}(m)$	3.057
Length of waterline	$L_{WL}(m)$	3.0901
Beamat waterline	$B_{WL}(m)$	0.4280
Draft	$D(m)$	0.1435
Displacement	$\Delta(m^3)$	0.1222
Blockcoefficient	C_B	0.651
Shipwettedareawithrudder	$S\ (m^2)$	1.6834
Longitudinalcentreofbuoyancy	$\%L_{BP}$,fwd+	-1.48
Themetacentricheight	$GM(m)$	0.008

Radiusof gyration	K_{xx}/B	0.49
Radiusof gyration	K_{yy}/L_{BP},K_{zz}/L_{BP}	0.25
Propeller diameter	$D_P(m)$	0.105
Propeller rotation direction (view from stern)		Right hand side
Rudder turn rate	(deg./s)	20.1
Froude number	Fr	0.095
Reynolds number	Re	1.25×10^6

Table2. The simulation cases

Case	Surge speed U_0(m/s)	Propeller rev. (RPS)	Depth / draft h/D	Free running simulations
0	0.518	6.75	1.20	20/5 zigzag, starting to port
				(Validation case)
1	0.518	6.75	1.20	Course keeping, 35°starboard turn
2	0.518	6.56	1.50	Course keeping, 35°starboard turn
3	0.518	6.43	2.00	Course keeping, 35°starboardturn
4	0.518	6.28	3.00	Course keeping, 35°starboard turn
5	0.518	6.24	4.00	Course keeping, 35°starboard turn
6	0.518	6.07	Deep water	Course keeping, 35°starboard turn

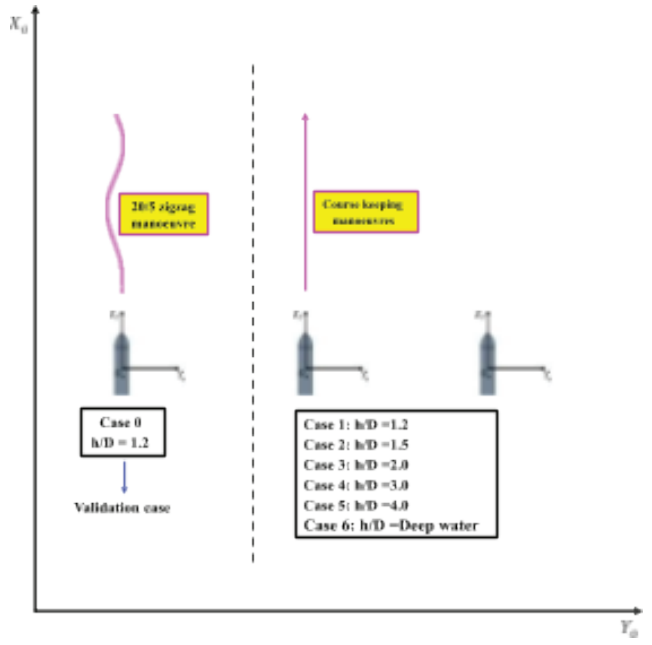

Figure 3: Graphic views of the simulation cases

3.2. Step2: "Numerical modelling"

The study employed the industrial CFD package STAR-CCM+, "version 15.04", for numerical simulations (Siemens, 2020). The numerical approach used in the study is detailed in this section. The main features of the approach are described, including the turbulence models, grid generation, boundary conditions, and numerical solution method. The aim was to make sure an adequate level of precision for the Computational Fluid Dynamics simulations and to capture the complexhydrodynamic phenomena occurring during the free-running maneuvers in shallow water.

The ship propeller was modeled using a finite-thickness actuator disk by means of the "body force method", incorporating both 'axial' and 'tangential' forces in the flow field within the disc to mimic propellorbehavior. The vessel used has a clockwise rotating,right-handed propeller,which propels the ship forward when seen from the aft of the ship. The simulations determined the direction of thrust produced by the disk model based on the characteristics of the right-handed propeller.

The computational domain was discretized using the Cartesian cut-cell method with the KCSmodel in STAR-CCM+. 6 separate grid generations were employed in the 'free-running' simulations, the precise number of which is listed in Table 3. The mesh density was refined in key areas such as around the hull body, between the rudder and horn, in the propeller wake region, and where the free surface was expected, to accurately capture complex flow features. A finer grid was specifically created between the ship hull and bottom boundary to properly resolve the hydrodynamic contact between the hull and seabed.

The CFD model's computational domain was divided into three regions: 1) background, 2) hull overset, and 3) rudder blade overset, as shown in Fig. 4. A dynamic "overlapping grid technique" was used for the last two regions to mimic the full 6 "degree-of-freedom" movements of the model and the rudder during the maneuvers. The dynamic overset approach allows independent handling of the movement of overset parts without restrictions. The gap spacing between the helm blade and root was marginally altered due to challenges in simulating the moving rudder in tight gap areas that mayhinder valid interpolations between meshes.

Table 3. The overall mesh figures for the 'free-running' models

Case no.	Total cell number
0 (h/D=1.2)	8,8 million
1 (h/D=1.2)	8,8 million
2 (h/D=1.5)	8,9 million
3 (h/D=2.0)	9,5 million
4 (h/D=3.0)	9,9 million
5 (h/D=4.0	10,2 million
6 (Deep water)	8,1 million

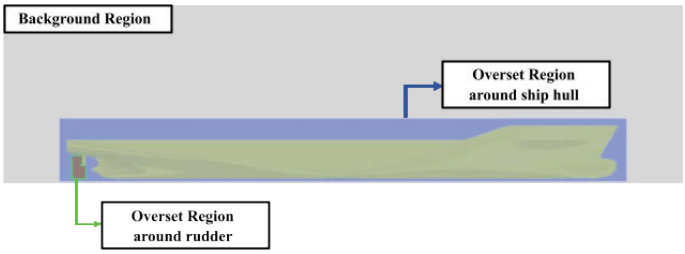

Figure 4: Illustration of the numerical domain for the 'free-running' CFD model

In this study, all free-running CFD simulations satisfied the Courant-Friedrichs-Lewy (CFL) condition by maintaining a CFL number less than 1 for numerical stability. The ITTC (2014) recommends using $\Delta t \leq 0.01$*Length/V for the time step (Δt) selection, with V being the ship speed.However, a more reliable level of accuracy for complex phenomena was achieved in this work by using a time step of $\Delta t=5x10^{-3}$ seconds, which is ten times smaller than the recommended value. The use of $\Delta t=5x10^{-3}$seconds has been proven to be reasonable in calculating the maneuverability of a '1÷75.24' scale containership model in question (as used in this work) through URANS-based simulations (Kim et al., 2021a).

The shallow water simulations (Case 0-5) used velocity inlet boundary conditions at the upstream, side, and top boundaries to avoid velocity gradients, and a pressure outlet at the downstream boundary. The bottom boundary was set as a stationary no-slip wall to represent the sea floor. Moving bodies (hull and rudder) had no-slip wall conditions. Toprevent wave reflection, wave damping witha length of 1.0 LBP was applied at the vertical boundaries. For 'deep-water' CFD model (Case 6), the only variation was the bottom boundary was set as a velocity inlet to represent deep water.

3.3.Step 3: Free running simulations

The 20/5 zigzag maneuver, the course keeping control, and the turning circle maneuver were performed for the KCS in this study. The control function for the modified 20/5 zigzag maneuver is as follows:

(1) $\min(kt,20)$,1st Rudder Execution$(t_1 \leq t \leq t_2)$

$\delta(t) = \{\max(20-k(t-t_2),-20)$,2nd Rudder Execution $(t_2 \leq t \leq t_3)$ $\min(-20 + k(t - t_3),20)$,3rd Rudder Execution $(t_3 \leq t \leq t_4)$

where t is the time passed after the beginning of each helm implementation, $\delta(t)$ is the helm angle,k isthemaximum helmrate (k= 20.1°/s).Theship was traveling straight atfull speed when therudder was first moved 20° to the port (1st rudder execution). This caused the ship to turn towards the port. When the ship had veered 5° off course, the rudder was moved 20° to the starboard (2nd rudder execution). This made the ship turn towards the starboard, slowing down its port ward turning until it reversed direction. Finally, when the ship reached 5° towards the right-hand side, the helm was moved back to the left-hand side (3rd helm implementation).

A control module was designed to assess the ship's course-keeping ability:

(2) $$\delta(t) = K_p e(t) + K_i \int_0^t e(t)dt + K_d \frac{de(t)}{dt}$$

(3) $$e(t) = \psi(t) - \psi_c$$

where $\psi(t)$ is the sudden yaw position at a particular time, ψ_c is the target yaw position which was defined at zero degrees to hold the vessel in course. K_p,K_i, and K_d denote the relative, integral, and derivative "control gains", in that order. In this numerical set-up, the "control gains" were calculated by means of the "trial-and-error method" ($K_p = 5, K_i = 0.05, and\ K_d = 3$). It is worth mentioning that the turning circle maneuver uses highest helm deflection (thirty-five degrees) to the right-hand side at highest helm rate and keeps the capacity rudder angle steady till the maneuver ends.

4. RESULTS

In allcaseslisted in Table 2, the methodology's steps 1-3 were applied to the KCS model. Readers can refer to Kim et al. (2022) for validation and verification.

4.1.Course keeping control

Shipsin waters usuallygoalongwith asteering pathof straight-line routes (set bya captain as well as navigators) not including for evasive maneuvers or planned course changes. This highlights the importance of evaluating a ship's ability to maintain a straight course, making it crucial to assess course-

keeping behavior under various sea conditions for safe navigation.

The results of the course-keeping simulations are displayed in Fig. 5, showing the ship's actual path compared to the target course. The deviations are small, indicating good "course-keeping" capability in the absence of outside factors for instance gusts, seas, and tides (Kim et al., 2021b). Table 4 summarizes the average quantities of "approach speed", drag, vertical ship movements at the maneuver. The ship's heading was kept close to 0°, with rudder deflection angles within 2.0° due to the asymmetric flow field caused by the propeller. The effect of water depth on resistance was shown to increase as the proportion of depth to draft decreases, together with the resistance in shallow water being 59% higher than in deep water. The ship experienced only minor heave and pitch motion due to its low approach speed.

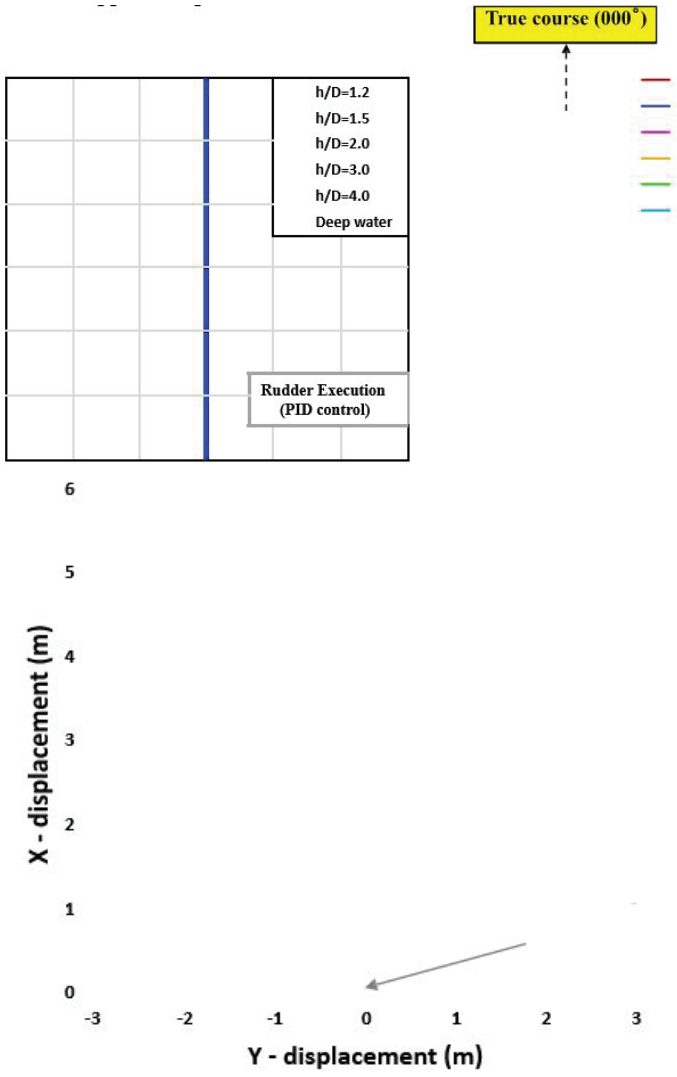

Figure 5: Evaluation of the paths practiced by the vessel in question at the "course keeping manoeuvre"

Table 4. The average quantities of the "approach speed", drag, vertical movements at the "course keeping" maneuver

Case no.	"Approach speed" U_0 (m/s)	Drag (Newton)	Heave (meters)	Pitch (deg)
1(h/D=1.2)	0.518	1.913	0.0033	0.165
2(h/D=1.5)	0.518	1.669	0.0024	0.166
3(h/D=2.0)	0.518	1.474	0.0017	0.169
4(h/D=3.0)	0.518	1.367	0.0011	0.172
5(h/D=4.0)	0.518	1.323	0.0008	0.172
6 (Deep water)	0.518	1.204	0.0004	0.171

4.2. Turning circle maneuver

Here in the current subsection, the turning capability of the self-propelled containership model in question will be evaluated in shallow waters, compared to its characteristic turning capability in calm, open water. The impact of restricted depths on maneuvering performance will also be analyzed. The standard turning circle maneuver involves the ship sailing forward under 'self-propulsion', then the helm being deflected to a hard-over angle of thirty-five degrees to the starboard side, at a maximum rate of twenty point one °/s. This causes the vessel to turn in the right-side path. The simulations end when the ship's heading angle reaches 360°, as per the procedure outlined by IMO (2002). The simulation time varies based on the ship's yaw velocity during the maneuver. The ship's turning behaviorisassessed usingstandard factors such as 'advance', 'transfer','tacticaldiameter', and 'time' to '90°/180° heading' changes.

The turning circle maneuver's predicted ship trajectories are shown in Fig. 6, using the "earth-fixed coordinate system" with the origin point being the position where the rudder was applied. The results of the maneuver parameters are presented in Table 5 to quantify the ship's turning quality for every case. The effect of restricted depth on the ship's turning operation may be seen from the differences in the turning path. The vessel's turning capability was poorer in restricted waters in this paper at ports defined with different water depths (h/D=1.2, 1.5, 2.0) than in open water. In spite of the like velocity (Froude number is 0.095), the vessel had greater "tactical diameters" (Figure 6 and Table 5) due to inadequate "Under Keel Clearance" (the distance among the ship's lowest point and the seabed), causing powerful hydrodynamic contact with the seabed and altering the ship's turning performance. The lesser the "Under Keel Clearance", the larger the vessel's "turning diameter". However, the vessel's maneuvering in restricted waters with the ratio of water depth to the vessel depth three and four was identical to deep water, indicating that the restricted water effect on the vessel's maneuverability weakened when the

above-mentioned ratio was larger than three.

According to Yeo et al. (2016), the impact of shallow water on a ship's turning performance was studied through "free-running" tank tests of the KVLCC2 in restricted waters (h/D=1.2, 1.5, and 2.0). The findings are given below:

1. Turning maneuvers resulted in a slower change in the ship's heading angle in shallower water depths.

2. The ship performing turning maneuvers experienced increasing hydrodynamic forces as the proportion of water depth to draught reduced exponentially.

3. Smaller h/D ratios were found to result in increased turning parameters such as ship advance, transfer, and tactical diameter transfer, and tactical diameter.

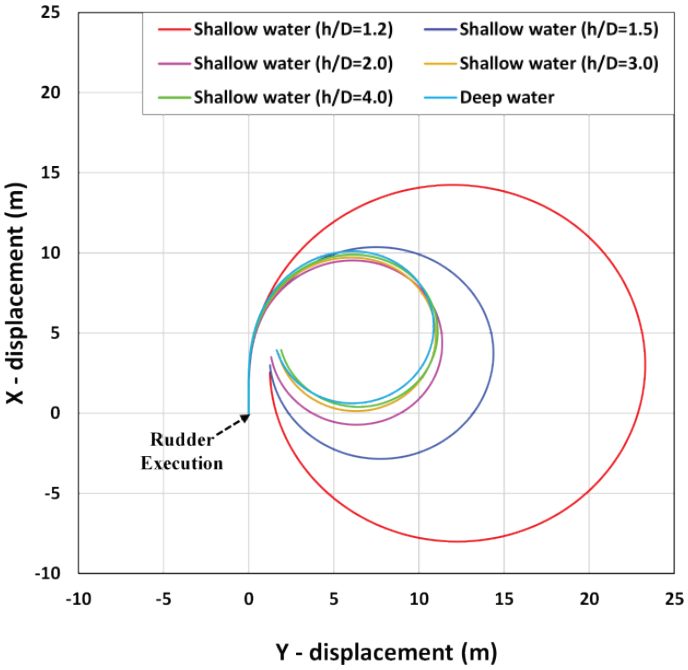

Figure 6: The simulated turning paths for each case

Table 5. Numerical outcomes for the turning factors

Parameters (CFD results)	*Case 1 (h/D = 1.2)*	*Case 2 (h/D = 1.5)*	*Case 3 (h/D = 2.0)*	*Case 4 (h/D = 3.0)*	*Case 5 (h/D = 4.0)*	*Case 6 (Deep)*
Advance (m)	14.23 **(4.66 L_{BP})**	10.33 **(3.38 L_{BP})**	9.45 **(3.09 L_{BP})**	9.57 **(3.13 L_{BP})**	9.73 **(3.18 L_{BP})**	9.89 **(3.24 L_{BP})**
Transfer (m)	11.56 **(3.78 LBP)**	6.82 **(2.23 L_{BP})**	5.16 **(1.69 L_{BP})**	4.80 **(1.57 L_{BP})**	4.80 **(1.57 L_{BP})**	4.65 **(1.52 L_{BP})**
Time for yaw 90 degrees (s)	47.24	32.51	27.97	27.64	27.92	28.04
Tactical diameter (m)	23.28 **(7.62 L_{BP})**	14.34 **(4.69 L_{BP})**	11.29 **(3.69 L_{BP})**	10.85 **(3.55 L_{BP})**	10.94 **(3.58 L_{BP})**	10.67 **(3.49 L_{BP})**
Time for yaw 180 degrees (s)	93.88	64.51	55.38	54.49	54.78	55.21

5. CONCLUSIONS

This study showed the effectiveness of using a direct CFD model, with an unsteady Reynolds Averaged Navier-Stokes solver, to estimate the maneuvering operation of a benchmarking model at ports which were defined using various water depths. Key findings:

1. The maneuvering vessel at ports (i.e., in restricted waters) exhibited reasonably well "course- keeping control", asshown by its realsailingcoursesbeingsteady with therealcourse. This indicates that the restricted depths have little impact on "course keeping" when there are no outside disturbances such as waves.

2. The study emphasized the impact of restricted depth on the ship's turning behavior by comparing the so-called "critical turning" factors and hydrodynamic properties with h/D ratios. Decreasing h/D led to increased "ship advance", "transfer", and "tactical diameter". For h/D = 1.2, the predicted transfer and tactical diameter were more than double those for open water, for the identical "approach speed" (Froude number is 0.095). No significant difference was found in the "turning parameters" between h/D= 3.0, 4.0, and open water, indicating negligible impact on the ship's maneuvering performance in these particular depths.

3. Deeper depths resulted in larger "involuntary speed loss" during the transitory stage of

theturn due to increased drag with heightened drift angle. "Speed loss rate (between initial surge velocity and minimum value) was 57% for h/D = 1.2, 64% for h/D = 1.5, 68% for h/D = 2.0, 70% for h/D = 3.0, 71% for h/D = 4.0, and 72% for deep water" (Kim et al., 2022).

4. The stream area faced by the maneuvering vessel was analyzed, revealing complex connections between the "hull wake", "boundary layer", "propeller", "vortex", and sea bottom (Kim et al., 2022).

6. ACKNOWLEDGMENTS

"It should be noted that the results were obtained using the ARCHIE-WeSt High-Performance Computer (www.archie-west.ac.uk) based at the University of Strathclyde". The full version of this paper was published in Applied Ocean Research (Kim et al., 2022) where the results presented in this paper were taken from.

7. REFERENCES

1. IMO, "Explanatory Notes to the standards for ship manoeuvrability", 2002.

2. ITTC, "ITTC - Recommended Procedures and Guidelines: Practical Guidelines for Ship CFD Applications", 2014

3. Kim, D., Song, S., Jeong, B., Tezdogan, T., "Numerical evaluation of a ship's manoeuvrability and course keeping control under various wave conditions using CFD". Ocean Engineering 237, 2021a, 109615.

4. Kim, D., Song, S., Jeong, B., Tezdogan, T., Incecik, A., "Unsteady RANS CFD simulations of ship manoeuvrability and course keeping control under various wave height conditions". Applied Ocean Research 117, 2021b, 102940.

5. Kim, D., Tezdogan, T., Incecik, A., "Hydrodynamic analysis of ship manoeuvrability in shallow water using high-fidelity URANS computations". Applied Ocean Research 123, 2022, 103176.

6. Siemens, Simcenter STAR-CCM+Documentation, 2020.

7. Tezdogan, T., Incecik, A., Turan, O., "Full-scale unsteady RANS simulations of vertical ship motionsin shallow water". Ocean Engineering 123, 2016, 131-145.

8. Yeo, D., Yun, K., Kim, Y., "Experimental study on the manoeuvrability of KVLCC2 in shallow water", 4th MASHCON-International Conference on Ship Manoeuvring in Shallow and Confined Water with Special Focus on Ship Bottom Interaction, 2016, pp. 287-294.